Journal of Cerebral Blood Flow & Metabolism (2010) 30, 703–717

www.jcbfm.com

Review Article

Use of magnetic resonance imaging to predict outcome after stroke: a review of experimental and clinical evidence

Tracy D Farr[1] and Susanne Wegener[2]

[1]*In-Vivo-NMR Laboratory, Max-Planck-Institute for Neurological Research, Cologne, Germany;* [2]*Department of Neurology, University Hospital Zurich, Zurich, Switzerland*

Despite promising results in preclinical stroke research, translation of experimental data into clinical therapy has been difficult. One reason is the heterogeneity of the disease with outcomes ranging from complete recovery to continued decline. A successful treatment in one situation may be ineffective, or even harmful, in another. To overcome this, treatment must be tailored according to the individual based on identification of the risk of damage and estimation of potential recovery. Neuroimaging, particularly magnetic resonance imaging (MRI), could be the tool for a rapid comprehensive assessment in acute stroke with the potential to guide treatment decisions for a better clinical outcome. This review describes current MRI techniques used to characterize stroke in a preclinical research setting, as well as in the clinic. Furthermore, we will discuss current developments and the future potential of neuroimaging for stroke outcome prediction.
Journal of Cerebral Blood Flow & Metabolism (2010) **30,** 703–717; doi:10.1038/jcbfm.2010.5; published online 20 January 2010

Keywords: stroke; magnetic resonance imaging; perfusion; diffusion; fMRI; outcome prediction

Introduction

Stroke is the third leading cause of death and the leading cause of disability in developed countries globally. The major obstacle to effective acute stroke management is time. It is estimated that fewer than 10% of all stroke patients receive the only approved treatment, thrombolysis with recombinant tissue plasminogen activator (rtPA; Cocho *et al*, 2005). There are several reasons for this, the primary of which is that thrombolysis is only approved for use within 3 h after symptom onset, although recent studies have suggested benefit beyond that from 4.5 (Hacke *et al*, 2008) to as long as 6 h (Davis *et al*, 2008; Rother *et al*, 2002). Other potential reasons include lack of public awareness, intrahospital delays, or precaution on account of the increased risk (7%) of intracerebral hemorrhage (ICH) that accompanies rtPA (Bambauer *et al*, 2006; Kleindorfer *et al*, 2004). In addition, it is controversial whether small vessel occlusions (lacunar stroke) respond as well to thrombolysis as territorial strokes (Cocho *et al*, 2006; Hsia *et al*, 2003; Hwang *et al*, 2008; rtPA for minor strokes: the National Institute of Neurological Disorders and Stroke rt-PA Stroke Study Experience, 2005). Nevertheless, when successful, early recanalization is highly correlated with reduced infarct volume and improved outcome scores (Felberg *et al*, 2002; Uchino *et al*, 2005). Because acute neuroimaging is not consistently performed, it is difficult to estimate the number of patients that exhibit spontaneous recanalization. Reports vary between 77% in patients with cortical infarcts using computed tomography (CT) and 32% in patients with middle cerebral artery occlusion (MCAO), using magnetic resonance angiography (MRA; Jorgensen *et al*, 1994; Neumann-Haefelin *et al*, 2004). Clearly, the heterogeneity of the patient population makes the decision to treat a difficult one. Therefore, effective neuroimaging strategies are essential to improve the standard of patient care.

Although CT is still the most prevalent imaging modality in acute stroke, magnetic resonance

Correspondence: Dr S Wegener, Department of Neurology, University Hospital Zurich, Frauenklinikstrasse 26, 8091 Zurich, Switzerland.
E-mail: Susanne.Wegener@usz.ch
This work was supported by grants from the StemStroke EU-FP6 program (LSHB-CT-2006-037526), Alexander von Humboldt Research Fellowship (to TDF), the European Commission (Marie-Curie Outgoing International Fellowship), the Department of Neurology, University Hospital Zurich, Switzerland, and by the NCCR 'Neural Plasticity and Repair' of the Swiss National Science Foundation (to SW).
Received 21 July 2009; revised 23 December 2009; accepted 4 January 2010; published online 20 January 2010

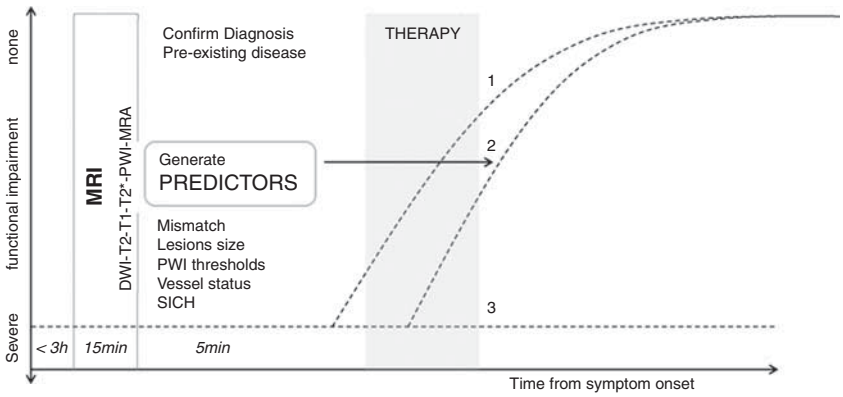

Figure 1 Magnetic resonance imaging (MRI)-guided stroke therapy. Three clinical scenarios are indicated in this diagram: (1) spontaneous improvement, (2) improvement in response to therapy, and (3) no spontaneous improvement or response to therapy. Only in scenario 2 is therapy really effective, whereas side effects could worsen outcome in 1 and 3.

imaging (MRI) is starting to measure up. The slightly longer acquisition times required for MRI represent a disadvantage. However, in less than 15 mins several different scans can be obtained that provide much more information regarding different tissue parameters. Magnetic resonance imaging can identify preexisting lesions and/or diseases, locate the thrombus, recognize ICH, classify stroke subtype, assess blood supply, and provide information about the approximate time of ischemia onset and the extent of injury. The function of MRI in acute stroke is to confirm the clinical diagnosis and to assess the risks and benefits for therapy. In an ideal situation, MRI would provide information that would assist with stratification of patients based on most likely outcome. In the acute clinical setting, important scenarios to differentiate for the clinician are: (1) spontaneous improvement, (2) improvement with therapy, and (3) no improvement despite therapy (Figure 1). In this review, we describe the MRI techniques currently used as surrogate markers and predictors of outcome in patients and experimental animal models of stroke. Future challenges of MRI-based outcome prediction in stroke will be discussed.

Surrogates for outcome assessment

One of the key issues in stroke assessment is how to best choose study end points that appropriately indicate outcome. Ideally, the end point should reflect the functional impairments caused by the disease and/or their effect on the quality of life. Therefore, the most common end points in the clinic are neurologic scales. Several neurologic scales have been used as surrogates for outcome, among them the modified Rankin scale, Glasgow Outcome Scale, and Barthel Index (Kasner, 2006). The modified Rankin scale and Glasgow Outcome Scale are used as indicators of functional independence for daily activities; and although both have been shown to be extremely reliable and reproducible (Banks and Marotta, 2007), they are not as comprehensive as the Barthel Index, which provides a more detailed examination of self-care abilities (Sulter *et al*, 1999). However, these measures are usually only performed out to 3 months because most spontaneous recovery is maximal by 10 weeks (Schiemanck *et al*, 2006). Therefore, these outcome surrogates have not been sufficiently studied long term, despite the fact that the aged brain may be capable of recovery many years after stroke.

In experimental animal research functional outcome surrogates are referred to as behavioral testing. Unfortunately, as most end point measures are collected within the first week of the ischemic event it is difficult to identify potential surrogates of functional outcome in the chronic setting. Nevertheless, several approaches have been used to assess functional outcome. A wide range of neurologic scores have been developed that attempt to mimic the clinical situation. They range from a simple 0 to 5 score based primarily on forelimb retraction (Bederson *et al*, 1986) to a slightly more detailed assessment that includes sensory response to stimuli (Garcia *et al*, 1995). Often this approach is preferred because neurologic scores are easy to perform, fast, and require very little equipment or expertise. However, the scores are not particularly sensitive to specific functional impairments and animals show a great deal of recovery. Other tests are designed to maximize the difference between the intact and impaired side of the body, typically, sensory capabilities of the forepaws. These are collectively referred to as asymmetry tests (Barth *et al*, 1990; Schallert *et al*, 2000). Ideally, tests designed to monitor skilled motor function in rodents should provide better comparability to the clinical situation. Challenging tests for skilled motor function exist, for example, skilled reaching for food in trays, on staircases (Montoya *et al*, 1991), or single food items (Whishaw *et al*, 1992). However, the highly labor-intensive and

interpretive nature of these tests means they are often excluded from the literature.

Imaging surrogates

Infarct Size

Magnetic-resonance-assessed final infarct size has been consistently used as an outcome surrogate based on the notion that the size of the insult is correlated with outcome severity. Indeed, a recent meta-analysis of the clinical literature—not part of any randomized clinical trial—reported a correlation between MRI-based lesion size and functional outcome parameters (Schiemanck *et al*, 2006). This analysis included studies that used several different methods to estimate acute lesion size including diffusion and perfusion weighted imaging (DWI and PWI, respectively), as well as T_2-weighted imaging. The T_2-weighted volume estimations are typically smaller than the initial DWI or PWI lesion size calculations, and are more reliable for subacute and long-term detection than they are for acute detection. As such, they are often used as a surrogate for final infarct size (Kane *et al*, 2007). Diffusion weighted imaging and PWI for acute lesion size will be discussed later about their potential to predict final lesion size.

Despite the use of T_2-weighted imaging to estimate final infarct size, debate exists regarding whether it is the most reliable measure. Fluid attenuation inversion recovery (FLAIR) is superior to conventional T2-weighted imaging regarding lesion conspicuity in the subacute stages (Ricci *et al*, 1999) because of its high sensitivity to very small accumulations of fluid by effectively nulling the signal from the cerebral spinal fluid. Fluid attenuation inversion recovery is currently included into the routine clinical acquisition scan package. Furthermore, interrater agreement using fluid attenuation inversion recovery has been reported to be better than for T_2-weighted imaging (Neumann *et al*, 2009). Manual delineation is still the most common approach to estimate infarct size, despite the significant measurement error (Davis *et al*, 2008), because automated volumetry is confounded by preexisting disease, individual variances in shape, location, and severity of signal change.

Final infarct size has been used consistently as an outcome surrogate in the experimental animal setting. Infarct size has traditionally been measured with 2,3,5-triphenyltetra-zolium chloride, hematoxylin–eosin, or nissl-stained brain sections, though the increasing availability of MRI in the experimental research environment has started to produce studies in which T_2-weighted imaging has been used to estimate final infarct size (Ashioti *et al*, 2007; Farr *et al*, 2007; Palmer *et al*, 2001). Infarct sizes assessed by T_2-weighted imaging have been shown to correlate well by some (Palmer *et al*, 2001) and to underestimate histologic damage by others (Neumann-Haefelin *et al*, 2000). Unfortunately, infarct size has been the primary, and often only, end point measure collected in many experimental stroke studies for quite some time. There are hundreds of potential compounds/drugs that were perceived as potential neuroprotective agents because of their ability to reduce infarct size in rodent models of stroke. However, all have failed to provide any benefits in clinical trials, a comprehensive list of clinical drug trials can be found at the Stroke Trials Registry website of the Internet Stroke Centre (Goldberg). Some of the most popular examples that have made it to phase III clinical trials without evidence of clinical efficacy include glutamate antagonists (for example, Selfotel: Acute Stroke Studies Involving Selfotel Treatment) (Davis *et al*, 2000), sodium or calcium channel blockers (for example, Lubeluzole: Lubeluzole in Ischemic Stroke) (Diener *et al*, 2000), or the recently highly publicized free radical scavenger Cerovive: Stroke Acute Ischemic NXY-059 Treatment (SAINT I and II) (Diener *et al*, 2008). It is therefore likely that the criterion of infarct size alone is insufficient to be used as a sole outcome surrogate. Functional connectivity of adjacent brain regions can be affected by a stroke through retrograde degeneration between existing neuronal networks. This is not observable using infarct size estimations, but could be inferred with other imaging modalities.

Diffusion Tensor Imaging

Anisotropy is the direction-dependent diffusion of water, which is faster in the direction of fiber tracts than perpendicular to them. Therefore, diffusion tensor imaging (DTI) was developed to visualize the orientation and properties of white matter (Basser *et al*, 1994). In principle, DTI could thus be used to detect some degree of physical connectivity between brain regions, which could be used as an outcome surrogate in the long-term setting. Typically, DTI data are presented as two-dimensional fractional anisotropy (FA) maps. Although FA has consistently been shown to decrease after stroke as gray and white matter disintegrate (Buffon *et al*, 2005), some variability in FA has been observed acutely. Decreases (Morita *et al*, 2006; Zelaya *et al*, 1999) and increases (Bhagat *et al*, 2008; Ozsunar *et al*, 2004) have been observed, and though the exact mechanism of the increase remains unclear, it is possible that perpendicular diffusion is restricted hyperacutely. Recovery of FA values 3 years after stroke has been observed in the internal capsule of patients with upper limb impairments subjected to 30 days of motor training (Stinear *et al*, 2007). If a sufficient number of diffusion directions and gradient strengths are used, DTI data can be reconstructed as three-dimensional maps that are color coded for directional sensitivity and continuous virtual tracts can be traced based on the largest principal

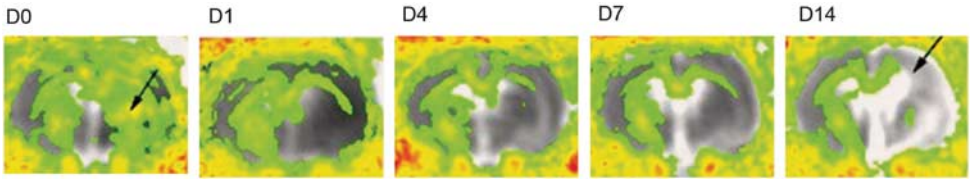

Figure 2 Changes in diffusion tensor imaging (DTI) in rats after transient middle cerebral artery occlusion (MCAO). Fractional anisotropy (FA) maps at different time points (D0–D14) averaged from eight animals, overlaid onto averaged apparent diffusion coefficient (ADC) maps. In the acute stages, there is a local FA increase (arrow on D0) in the ischemic territory. Subsequently, anisotropy decreases and fiber tracts degenerate ipsilateral to the lesion (arrow in D14). Corresponding ADC increases with tissue necrosis and liquefaction.

diffusivity between voxels (tractography). This strategy has been used to observe changes in the corticospinal tract after stroke (Moller *et al*, 2007) and to correlate DTI signals in certain fiber tracts of the ischemic hemisphere to the likelihood of outcome improvement (Pannek *et al*, 2009).

In agreement with the clinical reports, FA values also decrease in the ischemic territory of the rat brain over time (depicted in Figure 2). However, some groups have reported increases in FA values near the lesion boundary between 3 and 9 weeks after stroke (van der Zijden *et al*, 2008), which is enhanced with neural progenitor cell treatment (Jiang *et al*, 2006), as well as in the ipsilateral striatum around 21 days after stroke (Granziera *et al*, 2007). The latter two studies also used *ex vivo* DTI measurements to obtain tractography. Abnormal fiber trajectories were identified that originated in the ischemic and projected to the contralateral striatum in a small subset of animals with subcortical infarcts (Granziera *et al*, 2007), and increased numbers of tracts were observed projecting from the corpus callosum into the injured tissue (Jiang *et al*, 2006). However, conclusions regarding white matter reorganization must be interpreted cautiously on account of the sensitivity of the measurements and drawbacks with the analysis methods. In addition, the long acquisition times required for tractography represent a major drawback for *in vivo* experiments, particularly in the experimental animal setting. Scan times depend on resolution requirements, hardware capabilities, and sequence parameters. For example, to obtain an in-plane resolution of 400 μm^2 using 30 diffusion directions and a single gradient strength, acquisition time is estimated to be approximately 30 mins. This would double with each additional gradient strength and/or average. Time can also be gained with hardware improvements, for example, parallel imaging, which is common in the clinic, and future improvements in analysis strategies could increase the potential of DTI as an imaging surrogate.

Functional MRI

Connectivity between brain regions can also be inferred by measuring brain activity in stroke patients using functional MRI (fMRI). Depending on the kind of functional deficit, individual tasks can be designed to pinpoint where brain activity is impaired and how the ischemic brain has adapted to the injury, which makes fMRI a complementary imaging surrogate to infarct size measurements. As to reorganization of motor function after stroke, several general patterns of fMRI activity changes have been observed, reviewed elsewhere (Calautti and Baron, 2003; Carey and Seitz, 2007; Cramer and Bastings, 2000; Grefkes and Fink, 2009). Activity significantly increases in motor-related and peri-infarct areas, and tasks performed by the impaired hand produce bilateral cortical activation, including regions not activated in intact patients. The heterogeneity of the patient population requires stratification of lesion types to identify trends. Subcortical lesions often recruit independently connected cortical regions, whereas patients with cortical lesions show recruitment of peri-infarcted cortices. In general, recruitment of peri-infarct tissue is associated with improved recovery.

The availability of only a few stimulus/response fMRI paradigms in rodents means that this field is relatively unexplored in the preclinical research environment. The most well-characterized paradigm is the detection of either a cerebral blood flow (CBF) or blood-oxygen-level-dependent response in the primary somatosensory cortex (S1) after electrical stimulation of the forelimbs (Mandeville *et al*, 1998; Silva *et al*, 1999). In general, blood-oxygen-level-dependent and cerebral blood volume responses to forelimb stimulation are decreased after MCAO, and become more variable when compared with an intact response in healthy control animals (Butcher *et al*, 2005). However, a few groups have observed changes in the fMRI response, which correlate with the clinical literature. Stimulation of the impaired limbs produced activation in the intact sensorimotor cortex, and formerly unresponsive regions in the peri-infarcted tissue (Abo *et al*, 2001; Dijkhuizen *et al*, 2001; Rother *et al*, 2002). Interestingly, when repetitive fMRI sessions were performed in the same animals, three types of responders were characterized: those that retained, those that lost, and those that exhibited only a transient loss of the blood-oxygen-level-dependent response that was independent of infarct size measurements (Weber *et al*, 2008). As is the case with DTI, fMRI could offer

complimentary information to the standard infarct size estimations and could thus be considered a surrogate.

Outcome predictors

In contrast to surrogates, which are useful in the long-term setting to assess end point measures, outcome predictors are parameters that may be used in the acute setting of stroke to foresee the course of the disease or the potential benefit of treatment. Arguably the most common clinical predictor of outcome is the National Institutes of Health Stroke Scale (NIHSS), which is used in the acute stroke setting to assess a patient's neurologic symptoms. The National Institutes of Health Stroke Scale score has been shown to be highly correlated with differences in lesion size (Warach *et al*, 2000), and is an excellent predictor of outcome determined using the modified Rankin scale at 3 months (Johnston *et al*, 2009; Kasner, 2006). Ideally, as is the case with surrogates, additional predictors would be extremely useful and in this section we discuss several promising MRI predictors.

Magnetic Resonance Angiography

Magnetic resonance angiography is used acutely in the clinic for fast and effective diagnosis of acute stroke, primarily by identifying the location of the thrombus (Yu *et al*, 2002) and visualizing recanalization either spontaneously or in response to rtPA (Kimura *et al*, 2009). In terms of its predictive potential, MRA has been used to predict the degree of recanalization, which is highly correlated with outcome. The Thrombolysis In Myocardial Infarction grading system has been applied to assess the degree of the recanalization in patients with MCAOs using time-of-flight (TOF) MRA (Neumann-Haefelin *et al*, 2004). Patients with complete, and even minimal, recanalization exhibited significantly less lesion growth.

In addition to the success of recanalization therapies, MRA can be used to predict the risk of stroke by evaluating the degree of stenosis, and/or discrete changes in vessel walls, such as arteriovenous malformations or vasculitis (Kuker *et al*, 2008; reviewed in Latchaw *et al*, 2009). Although conventional intraarterial angiography is still the gold standard to evaluate the location and severity of vessel stenosis, the risks of this catheter-based procedure are significant. Imaging methods, such as ultrasound, can be preferred. Magnetic resonance angiography has been shown to be comparable and even superior to ultrasound for evaluating vessel stenosis (Nonent *et al*, 2004). In addition to TOF-MRA where blood flow is visualized noninvasively with short TR images, contrast-enhanced MRA (CE-MRA) is also routinely used. In CE-MRA, a Gadolinium bolus is injected intravenously and filling of the vessel lumen is recorded using T1-weighted images. Disadvantages of TOF-MRA when compared with CE-MRA are significantly longer scan times and less sensitivity to low flow, which potentially overestimates the degree of stenosis (Nederkoorn *et al*, 2003). Despite the recent suggestion that there is no greater benefit of CE-MRA (Babiarz *et al*, 2009), a meta-analysis has revealed that CE-MRA is slightly superior to TOF (Debrey *et al*, 2008). Another interesting application of MRA in stroke is its use to identify several characteristics of the atherosclerotic build up that could provide indications of plaque vulnerability (reviewed in Saam *et al*, 2007). For example, TOF was able to delineate the boundaries of the inflammatory fibrous cap rupture in atherosclerotic patients (Mitsumori *et al*, 2003), as well as fresh intraplaque hemorrhage (Yim *et al*, 2008). In addition, contrast agents, specifically ultrasmall superparamagnetic iron oxide nanoparticles, have been shown to accumulate inside the macrophages contained in the fibrous cap (Kooi *et al*, 2003), which could also enhance predictability of rupture potential.

Magnetic resonance angiography in the experimental setting can be used in much the same manner as the clinic, to determine thrombus location and recanalization, only when an embolic model is used (Hilger *et al*, 2002). However, the resolution is currently lacking to obtain images of smaller arteries or main stem branches, which makes implementation of MRA for examination of endothelial disease difficult. The most common model of MCAO in the rodent is the intraluminal filament technique, and model failure is a potential pitfall of this technique (Dittmar *et al*, 2005). Magnetic resonance angiography has been used to identify and exclude these animals earlier (Gerriets *et al*, 2004). Although use of MRA is limited in the experimental setting, development of new contrast agents for examination of atherosclerotic plaques can be tested easily.

Relaxometry

The susceptibility effects produced by iron in the blood appear as hypointensities in gradient echo images. Therefore, T_2^*-weighted images are used to identify ICH and or subarachnoid hemorrhage. It is generally accepted that CT is more accurate for ICH detection acutely (Warlow *et al*, 2003). However another study found that the two modalities were equivalent and that MRI was even slightly better (Kidwell *et al*, 2004). Indeed, a recent review regarding acute stroke imaging recommendations assessed the quality of articles based on level of evidence and suggested that the assumption that CT is more accurate for ICH detection than MR is based on a low level of evidence (Latchaw *et al*, 2009).

It has also been suggested that T_2^*-weighted MRI could be used to predict which patients might

exhibit secondary ICH (SICH) after an ischemic stroke (Nighoghossian *et al*, 2002). Preexisting hypointensities in T_2^*-weighted images are often classified as cerebral microbleeds, and regardless of their age could represent increased risk of SICH. As mentioned previously, these patients are often excluded from rtPA treatment, though the prognosis of SICH is not necessarily poor when compared with the potential impact of the initial ischemic event (Derex *et al*, 2004; von Kummer, 2002). Furthermore, recent evidence suggests that in fact these patients should not be excluded from rtPA treatment. The Bleeding Risk Analysis in Stroke by T_2^*-weighted Imaging before thromboLysis study revealed no increased risk of SICH from thrombolysis (Fiehler *et al*, 2007). In a recent study, fluid attenuation inversion recovery images were able to delineate focal regions of hyperintensity before thrombolysis that were highly correlated with increased risk of SICH (Cho *et al*, 2008) and could thus be used as an attractive SICH predictor.

In experimental animal research, gradient echo imaging is the most common technique for reliable detection of ICH (Neumann-Haefelin *et al*, 2001). However, reproducibility of images from day to day represents a major problem with this technique because of the difficulties associated with shimming across the small rodent brain. Another application for T_2^*-weighted images is the detection of susceptibility agents such as contrast agents. Systemic intravenous administration of ultrasmall superparamagnetic iron oxide nanoparticles for phagocytosis by activated blood-borne macrophages as a method to image the peripheral inflammatory response after stroke is one such application (Rausch *et al*, 2002; Wiart *et al*, 2007). However, evidence indicates this technique may not be so robust (Desestret *et al*, 2009; Henning *et al*, 2009), and more variability has been observed in the clinical setting (Cho *et al*, 2007; Nighoghossian *et al*, 2007; Saleh *et al*, 2007). Therefore, albeit offering interesting insights into the poststroke inflammatory reaction, the current potential of these techniques for stroke outcome prediction is poor.

Diffusion-Weighted Imaging

Many ischemic lesions are difficult to detect within 3 h using CT (Roberts *et al*, 2002), which has caused DWI to become the mainstay of acute stroke imaging (reviewed in Latchaw *et al*, 2009; Masdeu *et al*, 2006). Diffusion weighted imaging measures random mobility of water (protons) in tissue. Opposing magnetic field gradients first dephase and then rephase the proton spins. If no net movement has occurred, the signal is attenuated. However, if diffusion is restricted, for example, because of intercompartmental water shift produced by cytotoxic edema during acute stroke, the corresponding diffusion signal is hyperintense, and the quantitative apparent diffusion coefficient (ADC) values (mm^2/sec) decrease. Apparent diffusion coefficient maps more clearly discriminate cytotoxic edema from existing pathologic entities produced by the T_2-shine-through effect that can be observed in the DW images (Detre *et al*, 1994). In general, ADC values do not change much until CBF drops below 20 mL/100 g per min. Subsequently, the most severe ADC reductions are found in the center of the perfusion deficit, indicating that specific ADC values are able to discriminate between infarct or necrotic tissues, and thus predict tissue outcome (Kraemer *et al*, 2005; Thomalla *et al*, 2003). When regions of interest were drawn around the initial DWI abnormality (core) and again around the hyperintense T_2 region (final infarct size), both regions, as well as the difference between the two (tissue at risk), showed different ADC values: core, 0.56 ± 0.11; tissue at risk, 0.71 ± 0.11; and final infarct, $0.63 \pm 0.11 \times 10^{-3}\,mm^2$/sec (Na *et al*, 2004). The most severe ADC decreases (10^{-3} 0.45 to 0.7 $10^{-3}\,mm^2$/sec) are correlated with low cerebral metabolic rates of oxygen ($CMRO_2$) (0.4 to 0.5 μmol/100 mL per min), which is consistent with irreversible tissue damage (Guadagno *et al*, 2006). However, ADC values become much more variable in tissue with $CMRO_2$ levels that could be associated with either penumbra or benign oligemia (Guadagno *et al*, 2006). Furthermore, there have been a few reports where ischemic lesions were undetected with DWI (Lefkowitz *et al*, 1999; Wang *et al*, 1999), or that severe ADC decreases normalized, depending on the duration and severity of ischemia (Rother *et al*, 2002). Therefore, the ADC value of a voxel alone is not always sufficient to predict its fate. Recent automated postprocessing methods have tried to overcome this problem by incorporating regional ADC measures and local shape regularity constraints (Rosso *et al*, 2009). Lesion size estimated by DWI is often used to predict outcome as several studies have observed correlations with functional outcome scales (Barrett *et al*, 2009; Johnston *et al*, 2009), though it should be pointed out that a few studies have failed to find a correlation (Hand *et al*, 2006; Wardlaw *et al*, 2002).

As is the case in the clinic, ADC abnormalities are preferred for estimation of infarct size in animal research, and manual delineation showed a better correlation with 2,3,5-triphenyltetra-zolium chloride sections than threshold based estimations (Bratane *et al*, 2009). Nevertheless, several different thresholds have been used to correlate infarct size with histologic measurements. Apparent diffusion coefficient volumes, when expressed as threshold of 77% of control values, were highly correlated with measurements of reduced adenosine triphosphate and glucose consumption (breakdown of energy metabolism). Volumes determined with a threshold of 86% of control values were correlated with measurements of tissue acidosis 24 h later (Olah *et al*, 2001). An ADC decrease of 33% when compared with the contralateral side was also highly

correlated with hemispheric lesion volume at 3 h after MCAO (Kazemi *et al*, 2004). Another group used semiautomated software to delineate the lesion based on a combination of ADC and T_2-weighted abnormalities at various time points. Infarct size from hematoxylin–eosin sections was highly correlated with the measurements starting around 16 h after MCAO (Jacobs *et al*, 2000). If reperfusion occurs, the region of ADC abnormality will return to normal or near-normal values, and subsequent expansion in the subacute stages is variable (Li *et al*, 2000). The eventual extent of the ADC region by 24 h is highly correlated with occlusion duration (Neumann-Haefelin *et al*, 2000) and several groups have shown with histology that the signal is not solely confined to the neuronal population (Liu *et al*, 2001; Ringer *et al*, 2001). A recent review on the potential of DWI to predict infarct size accurately in experimental animal research indicated that there were only 13 reports that achieved quality scores sufficient to draw conclusions from. In general, manual delineation of lesion size from DWI was a better indicator of neuronal damage than lesions defined by using quantitative ADC thresholds (Rivers and Wardlaw, 2005). This implies that although quantitative ADC maps are crucial to diagnose acute ischemic damage unambiguously, ADC-defined thresholds may be too dynamic in the course of the disease to yield a robust outcome predictor.

Perfusion-Weighted Imaging

Perfusion-weighted imaging is of particular importance in stroke, as the drop in CBF (usually specified in mL/100 g per min) is one of the first in the cascade of events that ultimately result in brain damage. The extent, severity, and duration of the misery perfusion are a major determinant of outcome. In addition to confirming the diagnosis of stroke and indicating reperfusion, it has been shown that areas with severely compromised perfusion are more likely to undergo infarction, which makes PWI an interesting outcome prediction parameter (Butcher *et al*, 2003). When time of symptom onset is not certain, a persistent perfusion deficit on PWI can help stratify patients for therapy. Induced hypertension to avoid a remittance of symptoms because of low perfusion pressure after transient ischemia is also typically guided by PWI.

The most common clinical technique for PWI is dynamic susceptibility contrast (DSC) bolus tracking, which relies on intravenous administration of a contrast agent. The corresponding signal in the blood vessels, and surrounding parenchyma, is subsequently reduced (Villringer *et al*, 1988) and signal change over time can be used to calculate CBF, cerebral blood volume, and the average time required for any given particle of tracer to pass through the tissue after an ideal bolus injection, mean transit time (Barbier *et al*, 2001; Calamante *et al*, 1999; Ostergaard, 2005). Compared with the 'gold standard' of positron emission tomography (PET) imaging, DSC-derived CBF values have large standard deviations and tend to overestimate the hypoperfused tissue in stroke patients (Zaro-Weber *et al*, 2009). An inherent problem with DSC methods is that perfusion quantification algorithms rely on determining an arterial input function, which incorporates the concentration of the tracer over time in a voxel within a major artery, usually the middle cerebral artery. The input into this vessel, however, does not always resemble arterial input into the brain tissue, which can result in large and unsystematic errors (Calamante *et al*, 2002). In a recent comparison of different postprocessing algorithms and 10 different parameters of perfusion derived from bolus tracking it could be shown that (1) the choice of the parameter critically determines the ability to predict final infarct size and that (2) simple composite parameters such as the time-to-peak or first moment, resembling the arrival time of contrast in the voxel, might be superior to more sophisticated parameters that involve deconvolution of the arterial input function. A prolongation of first moment of 3.5 secs predicted infarction with a 75% sensitivity and 78% specificity (Christensen *et al*, 2009). Notably, MRI prediction was better in patients without reperfusion, indicating that, probably because of interindividual variance, perfusion thresholds might be even more difficult to determine on the verge of recanalization. In a different study, DSC perfusion maps were predictive of favorable clinical outcome to rtPA treatment when increasing the threshold for the delay of the time-to-peak residue function (T_{max}) (Olivot *et al*, 2009).

Recently, a noninvasive alternative has become popular in preclinical research, arterial spin labeling (ASL) (Detre *et al*, 1994; Williams *et al*, 1992). Pulsed ASL produces contrast by nonselectively, and then selectively, inverting endogenous protons. The resulting signal difference is proportional to the amount of inflowing protons, or CBF. Magnetically labeling blood means this technique is more robust in situations of blood–brain barrier disruption (Calamante *et al*, 2002). However, quantification can be difficult as assumptions of the quantification algorithms, such as arterial transit time, are difficult to predict in cerebrovascular disease states (Wegener *et al*, 2007). As the method is still fairly new and not yet implemented on many clinical scanners, data are lacking to test the predictive value of ASL-PWI in stroke patients. Regardless, promising novel methods, such as velocity-selective ASL (tagging blood based on velocity rather than location) (Wong, 2007) and arterial territory mapping (Hendrikse *et al*, 2009; van Laar *et al*, 2008) are promising and currently receiving a great deal of attention, as these methods may predict if a certain vessel stenosis is really of relevance for cerebral perfusion in the individual or if collateral blood supply is compensating sufficiently.

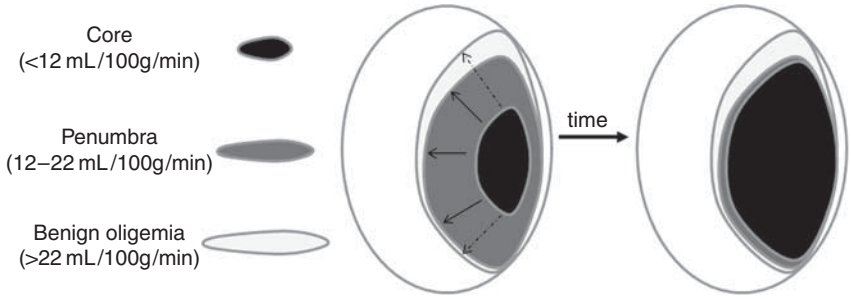

Figure 3 The penumbra. Cerebral blood flow (CBF) thresholds have been used to identify tissue that will exhibit irreversible damage (infarct core < 12 mL/100 g per min) and that could be salvageable (penumbra 12 to 22 mL/100 g per min) because some degree of metabolic activity remains. Theoretically, if CBF is not restored the core will gradually expand in the subacute stages as penumbral tissue dies. The magnetic resonance imaging (MRI)-defined diffusion/perfusion weighted imaging (DWI/PWI) 'mismatch' is the area of potential lesion growth. It is defined by the initial area of perfusion deficit (which usually includes the area of oligemia) minus the initial area with severe diffusion deficit (core). Growth of the core region can be variable (continuous or dashed arrows) depending on the defined DWI and CBF thresholds, reperfusion, and individual tissue resistance.

In rodent models of stroke, PWI has not been frequently performed, in part because it is hard to implement because of signal-to-noise constraints. In addition to DSC-based techniques, ASL approaches have been recently introduced to small animal stroke imaging (Leithner *et al*, 2008; Wegener *et al*, 2007). There has been less ambiguity as to the value of PWI in outcome prediction in animal models compared with the clinical setting, which is very likely explained by the homogeneity of vascular occlusions in animal models in contrast to patients (location, duration, clot composition and so on). Cerebral blood flow thresholds have been shown to be useful for infarct size prediction. Voxels with a CBF < 30 mL/100 g per min were very likely to be part of the 'core' and proceed to infarction despite reperfusion, if ADC values were reduced, too (Shen *et al*, 2003, 2004).

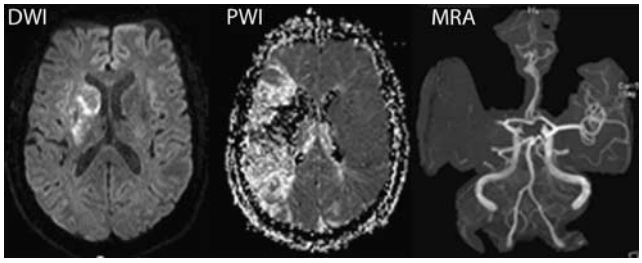

Figure 4 Identification of the diffusion/perfusion weighted imaging (DWI/PWI) mismatch. Diffusion-weighted images (left) and perfusion-weighted images (middle) in an 80-year-old patient at 8 h after the onset of acute aphasia, left-sided sensorimotor hemiparesis, and hemianopsia. *Note*: the small hyperintense lesion in DWI compared with the large area of hypoperfusion in PWI. Magnetic resonance angiography (MRA) reveals proximal occlusion of the left middle cerebral artery (kindly provided by J. Fiebach, Department of Neurology, Charité Universitätsmedizin Berlin).

The Mismatch Concept

Of central importance to stroke outcome is the concept of tissue at risk (Figure 3), which was only touched on in previous sections. Essentially, the region of brain most deprived of CBF (< 12 mL/100 g per min) is thought to be irreversibly damaged and destined for necrosis (infarct), whereas the surrounding areas retain some degree of CBF (12 to 22 mL/100 g per min) and thus represent a combination of tissue that will survive (oligemia) or whose fate is undecided depending on restoration of CBF (penumbra). Many different descriptions and classifications of these regions exist, reviewed elsewhere (Paciaroni *et al*, 2009; Sharp *et al*, 2000). Imaging-based identification of these regions is of great importance for outcome prediction and much effort has been made in this respect in the past decade.

Initial observations in patients that the region of DWI was smaller than the region of PWI abnormality lead to the development of the idea that the DWI/PWI 'mismatch' could be used to identify tissue at risk (Baird *et al*, 1997; Neumann-Haefelin *et al*, 1999). A DWI/PWI mismatch is illustrated in Figure 4. A perfusion deficit encompassing 120% of the size of the DWI lesion is generally accepted as a relevant mismatch (Sims *et al*, 2009). If the mismatch resembles a correlate of the real penumbra, two important conclusions should be possible with the detection of a large MRI-defined mismatch: (1) infarct growth if reperfusion is not achieved and (2) a large area of salvageable tissue. The latter suggests that patients with a large mismatch should respond better to thrombolytic treatment with rtPA, which has been shown even beyond the 3 h time window (Beaulieu *et al*, 1999; Lorenz *et al*, 2006; Ostergaard, 2005). However, the selection of patients for thrombolysis based on an MRI-defined mismatch is controversial (Fiebach and Schellinger, 2009; Schabitz, 2009). Although two phase II trials (the diffusion and perfusion imaging evaluation for understanding stroke evolution (DEFUSE) and the Echoplanar Imaging Thrombolytic Evaluation Trial (EPITHET)) have indicated that patients with a

mismatch might respond better to thrombolytic therapy, the DIAS-2 study did not show any benefit in patients selected for thrombolysis based on the existence of a mismatch (Albers *et al*, 2006; Davis *et al*, 2008; Donnan *et al*, 2009; Hacke *et al*, 2009). Of note, the mismatch in DIAS-2 was defined as a PWI lesion volume >20% of the DWI lesion volume by visual inspection at each participating stroke center. In DEFUSE and EPITHET, the mismatch (PWI/DWI lesion volume >1.2 and PWI/DWI lesion volume $\geqslant$10 ml) was determined by volumetric analysis at a later time point and did not influence stratification of patients into treatment groups. Although a systematic review ascertained that there is insufficient evidence to either provide or withhold thrombolytic treatment based on identification of a mismatch region (Kane *et al*, 2007), this is expected to change with the implementation of standardized, quantitative MRI analysis tools for '*ad hoc*' calculation of the mismatch before treatment.

As is clear from the previous section, there are many different methods in which to quantify CBF and the choice of which also impact estimation of the mismatch region. As such, there is no consensus regarding the best method to define the mismatch, which represents a problem regarding translation of findings between studies (Bandera *et al*, 2006). Recent advancements in techniques to estimate metabolic activity such as MRI-based assessment of $CMRO_2$ are expected to contribute to this (Xu *et al*, 2009), as well as combined machines such as MR/PET (Beyer and Pichler, 2009). With this technology it would be possible to perform simultaneous measurements, such as the oxygen extraction fraction with PET together with DWI/PWI mismatch to achieve a more precise estimate of the penumbra. Although good agreement has been shown between the relative distributions of the MRI-derived mismatch and the PET-derived penumbra, the mismatch is still prone to errors (Takasawa *et al*, 2008). Reasons include technical challenges regarding quantification of perfusion-weighted MRI, the fact that the lesion on DWI may recover and that areas with benign oligemia are included into the MRI-defined mismatch definitions (Guadagno *et al*, 2004; Heiss *et al*, 2004; Sobesky *et al*, 2004, 2005). In a study where PET was conducted roughly 1 h after MRI assessment of CBF (using the DSC bolus-tracking technique) in patients with acute ischemic stroke, a CBF threshold of <20 ml/100 g per min was found to best estimate hypoperfusion within the PET-derived penumbra (Zaro-Weber *et al*, 2009). The considerable interindividual variance, the influence of vessel disease, and the value of graded CBF ranges (e.g., 12 to 20 ml/100 g per min) for penumbra selection are areas of ongoing research in this field.

The concept of the mismatch has not been so extensively studied in animal stroke research. Mismatch regions have been reported in the acute stages of permanent MCAO, and in accordance with early clinical reports, the region of ADC abnormality gradually expands to encompass the region of perfusion deficit within the first 3 h (Bardutzky *et al*, 2007; Henninger *et al*, 2006; Meng *et al*, 2004). However, once CBF is restored in transient models, both DWI and PWI regions of abnormality are diminished and subsequent expansion is variable. In one study, core pixels were defined by a CBF decrease of more than 87% and an ADC decrease of more than 30%, whereas mismatch pixels were defined by a CBF decrease below and an ADC value above the defined thresholds (Bardutzky *et al*, 2007). Subsequent pixel fate was highly dependent on the duration of the MCAO. Durations of 35, 60, and 95 mins resulted in recovery of 46%, 28%, and 9% of the core pixels, respectively, whereas 85% of all mismatch pixels recovered regardless of occlusion duration. Again, quantification of these regions is highly dependent on the choices for thresholds, this can be further complicated by partial volume effects, which are present more frequently in high-resolution images (Ren *et al*, 2004). In addition, differences in the evolution of the mismatch region have also been reported to differ with experimental model (Henninger *et al*, 2006) and animal strain (Bardutzky *et al*, 2005), which are important considerations. As is the case with the clinic, alternative strategies may provide a more balanced perspective. For example, pH-weighted MRI applied to a DWI/PWI mismatch data set was able to identify regions that correspond to penumbra and benign oligemia (Sun *et al*, 2007). Combined PET/MRI (Judenhofer *et al*, 2008) and MRI/SPECT machines are increasingly used and also expected to make a contribution to a better characterization of the tissue at risk and tissue destined to undergo infarction in animal research.

Outlook

Magnetic resonance imaging can assist to predict the functional outcome of stroke patients. Several MRI parameters are correlated with a favorable outcome: (1) early recanalization on MRA, (2) small tissue defect on DWI, (3) small size and degree of perfusion deficit on PWI, (4) restored functional activity in peri-infarct areas on fMRI and intact descending pathways on DTI. However, the decision regarding whether a patient should receive thrombolysis solely based on MRI assessment remains problematic and controversial.

Many of the problems and open questions of stroke outcome prediction are similar in experimental animal research and in the clinic. However, the quality of preclinical research must be improved to make a better impact in the clinic. Low statistical power, flawed statistical interpretation, reproducibility, masking, randomization, quality control, and publication bias have all been suggested to contribute to the lack of effective translational stroke research (Dirnagl, 2006). Once preclinical knowledge is ready to be applied to patients, multicenter studies

are the only way to reach sufficient numbers for relevant conclusions, at which point standardization of MR acquisition and analysis strategies is essential. In addition, more long-term measures are required for ultimate evaluation of attempts at outcome prediction. Nevertheless, the field of experimental neuroimaging with MRI is rapidly expanding. Improvements in hardware and sequences that decrease scan time while maintaining resolution will continue to impact the field. Post-processing strategies must evolve to these increasingly complicated data sets. It also seems clear that multimodal imaging strategies are necessary to develop more detailed patient profiles that can be used to predict outcome. Magnetic resonance imaging prediction of stroke outcome and treatment response will remain an area of exciting research and a realistic goal for the next decade.

Conflict of interest

The authors declare no conflict of interest.

References

Abo M, Chen Z, Lai LJ, Reese T, Bjelke B (2001) Functional recovery after brain lesion—contralateral neuromodulation: an fMRI study. *Neuroreport* 12:1543–7

Albers GW, Thijs VN, Wechsler L, Kemp S, Schlaug G, Skalabrin E, Bammer R, Kakuda W, Lansberg MG, Shuaib A, Coplin W, Hamilton S, Moseley M, Marks MP (2006) Magnetic resonance imaging profiles predict clinical response to early reperfusion: the diffusion and perfusion imaging evaluation for understanding stroke evolution (DEFUSE) study. *Ann Neurol* 60:508–17

Ashioti M, Beech JS, Lowe AS, Hesselink MB, Modo M, Williams SC (2007) Multi-modal characterisation of the neocortical clip model of focal cerebral ischaemia by MRI, behaviour and immunohistochemistry. *Brain Res* 1145:177–89

Babiarz LS, Romero JM, Murphy EK, Brobeck B, Schaefer PW, Gonzalez RG, Lev MH (2009) Contrast-enhanced MR angiography is not more accurate than unenhanced 2D time-of-flight MR angiography for determining > or = 70% internal carotid artery stenosis. *AJNR Am J Neuroradiol* 30:761–8

Baird AE, Benfield A, Schlaug G, Siewert B, Lovblad KO, Edelman RR, Warach S (1997) Enlargement of human cerebral ischemic lesion volumes measured by diffusion-weighted magnetic resonance imaging. *Ann Neurol* 41:581–9

Bambauer KZ, Johnston SC, Bambauer DE, Zivin JA (2006) Reasons why few patients with acute stroke receive tissue plasminogen activator. *Arch Neurol* 63:661–4

Bandera E, Botteri M, Minelli C, Sutton A, Abrams KR, Latronico N (2006) Cerebral blood flow threshold of ischemic penumbra and infarct core in acute ischemic stroke: a systematic review. *Stroke* 37:1334–9

Banks JL, Marotta CA (2007) Outcomes validity and reliability of the modified Rankin scale: implications for stroke clinical trials: a literature review and synthesis. *Stroke* 38:1091–6

Barbier EL, Silva AC, Kim SG, Koretsky AP (2001) Perfusion imaging using dynamic arterial spin labeling (DASL). *Magn Reson Med* 45:1021–9

Bardutzky J, Shen Q, Henninger N, Bouley J, Duong TQ, Fisher M (2005) Differences in ischemic lesion evolution in different rat strains using diffusion and perfusion imaging. *Stroke* 36:2000–5

Bardutzky J, Shen Q, Henninger N, Schwab S, Duong TQ, Fisher M (2007) Characterizing tissue fate after transient cerebral ischemia of varying duration using quantitative diffusion and perfusion imaging. *Stroke* 38:1336–44

Barrett KM, Ding YH, Wagner DP, Kallmes DF, Johnston KC (2009) Change in diffusion-weighted imaging infarct volume predicts neurologic outcome at 90 days: results of the Acute Stroke Accurate Prediction (ASAP) trial serial imaging substudy. *Stroke* 40:2422–7

Barth TM, Jones TA, Schallert T (1990) Functional subdivisions of the rat somatic sensorimotor cortex. *Behav Brain Res* 39:73–95

Basser PJ, Mattiello J, LeBihan D (1994) MR diffusion tensor spectroscopy and imaging. *Biophys J* 66: 259–267

Beaulieu C, de Crespigny A, Tong DC, Moseley ME, Albers GW, Marks MP (1999) Longitudinal magnetic resonance imaging study of perfusion and diffusion in stroke: evolution of lesion volume and correlation with clinical outcome. *Ann Neurol* 46:568–78

Bederson JB, Pitts LH, Tsuji M, Nishimura MC, Davis RL, Bartkowski H (1986) Rat middle cerebral artery occlusion: evaluation of the model and development of a neurologic examination. *Stroke* 17:472–6

Beyer T, Pichler B (2009) A decade of combined imaging: from a PET attached to a CT to a PET inside an MR. *Eur J Nucl Med Mol Imaging* 36(Suppl 1):S1–2

Bhagat YA, Hussain MS, Stobbe RW, Butcher KS, Emery DJ, Shuaib A, Siddiqui MM, Maheshwari P, Al-Hussain F, Beaulieu C (2008) Elevations of diffusion anisotropy are associated with hyper-acute stroke: a serial imaging study. *Magn Reson Imaging* 26:683–93

Bratane BT, Bastan B, Fisher M, Bouley J, Henninger N (2009) Ischemic lesion volume determination on diffusion weighted images vs. apparent diffusion coefficient maps. *Brain Res* 1279:182–8

Buffon F, Molko N, Herve D, Porcher R, Denghien I, Pappata S, Le Bihan D, Bousser MG, Chabriat H (2005) Longitudinal diffusion changes in cerebral hemispheres after MCA infarcts. *J Cereb Blood Flow Metab* 25:641–50

Butcher K, Parsons M, Baird T, Barber A, Donnan G, Desmond P, Tress B, Davis S (2003) Perfusion thresholds in acute stroke thrombolysis. *Stroke* 34:2159–64

Butcher KS, Parsons M, MacGregor L, Barber PA, Chalk J, Bladin C, Levi C, Kimber T, Schultz D, Fink J, Tress B, Donnan G, Davis S (2005) Refining the perfusion–diffusion mismatch hypothesis. *Stroke* 36:1153–9

Calamante F, Thomas DL, Pell GS, Wiersma J, Turner R (1999) Measuring cerebral blood flow using magnetic resonance imaging techniques. *J Cereb Blood Flow Metab* 19:701–35

Calamante F, Gadian DG, Connelly A (2002) Quantification of perfusion using bolus tracking magnetic resonance imaging in stroke: assumptions, limitations, and potential implications for clinical use. *Stroke* 33:1146–51

Calautti C, Baron JC (2003) Functional neuroimaging studies of motor recovery after stroke in adults: a review. *Stroke* 34:1553–66

Carey LM, Seitz RJ (2007) Functional neuroimaging in stroke recovery and neurorehabilitation: conceptual issues and perspectives. *Int J Stroke* 2:245–64

Cho AH, Kim JS, Kim SJ, Yun SC, Choi CG, Kim HR, Kwon SU, Lee DH, Kim EK, Suh DC, Kang DW (2008) Focal fluid-attenuated inversion recovery hyperintensity within acute diffusion-weighted imaging lesions is associated with symptomatic intracerebral hemorrhage after thrombolysis. *Stroke* 39:3424–6

Cho TH, Nighoghossian N, Wiart M, Desestret V, Cakmak S, Berthezene Y, Derex L, Louis-Tisserand G, Honnorat J, Froment JC, Hermier M (2007) USPIO-enhanced MRI of neuroinflammation at the sub-acute stage of ischemic stroke: preliminary data. *Cerebrovasc Dis* 24:544–6

Christensen S, Mouridsen K, Wu O, Hjort N, Karstoft H, Thomalla G, Rother J, Fiehler J, Kucinski T, Ostergaard L (2009) Comparison of 10 perfusion MRI parameters in 97 sub-6-hour stroke patients using voxel-based receiver operating characteristics analysis. *Stroke* 40:2055–61

Cocho D, Belvis R, Marti-Fabregas J, Molina-Porcel L, Diaz-Manera J, Aleu A, Pagonabarraga J, Garcia-Bargo D, Mauri A, Marti-Vilalta JL (2005) Reasons for exclusion from thrombolytic therapy following acute ischemic stroke. *Neurology* 64:719–20

Cocho D, Belvis R, Marti-Fabregas J, Bravo Y, Aleu A, Pagonabarraga J, Molina-Porcel L, Diaz-Manera J, San Roman L, Martinez-Lage M, Martinez A, Moreno M, Marti-Vilalta JL (2006) Does thrombolysis benefit patients with lacunar syndrome? *Eur Neurol* 55:70–3

Cramer SC, Bastings EP (2000) Mapping clinically relevant plasticity after stroke. *Neuropharmacology* 39:842–51

Davis SM, Lees KR, Albers GW, Diener HC, Markabi S, Karlsson G, Norris J (2000) Selfotel in acute ischemic stroke : possible neurotoxic effects of an NMDA antagonist. *Stroke* 31:347–54

Davis SM, Donnan GA, Parsons MW, Levi C, Butcher KS, Peeters A, Barber PA, Bladin C, De Silva DA, Byrnes G, Chalk JB, Fink JN, Kimber TE, Schultz D, Hand PJ, Frayne J, Hankey G, Muir K, Gerraty R, Tress BM, Desmond PM (2008) Effects of alteplase beyond 3 h after stroke in the Echoplanar Imaging Thrombolytic Evaluation Trial (EPITHET): a placebo-controlled randomised trial. *Lancet Neurol* 7:299–309

Debrey SM, Yu H, Lynch JK, Lovblad KO, Wright VL, Janket SJ, Baird AE (2008) Diagnostic accuracy of magnetic resonance angiography for internal carotid artery disease: a systematic review and meta-analysis. *Stroke* 39:2237–48

Derex L, Nighoghossian N, Hermier M, Adeleine P, Philippeau F, Honnorat J, Yilmaz H, Dardel P, Froment JC, Trouillas P (2004) Thrombolysis for ischemic stroke in patients with old microbleeds on pretreatment MRI. *Cerebrovasc Dis* 17:238–41

Desestret V, Brisset JC, Moucharrafie S, Devillard E, Nataf S, Honnorat J, Nighoghossian N, Berthezene Y, Wiart M (2009) Early-stage investigations of ultrasmall superparamagnetic iron oxide-induced signal change after permanent middle cerebral artery occlusion in mice. *Stroke* 40:1834–41

Detre JA, Zhang W, Roberts DA, Silva AC, Williams DS, Grandis DJ, Koretsky AP, Leigh JS (1994) Tissue specific perfusion imaging using arterial spin labeling. *NMR Biomed* 7:75–82

Diener HC, Cortens M, Ford G, Grotta J, Hacke W, Kaste M, Koudstaal PJ, Wessel T (2000) Lubeluzole in acute ischemic stroke treatment: a double-blind study with an 8-hour inclusion window comparing a 10-mg daily dose of lubeluzole with placebo. *Stroke* 31:2543–51

Diener HC, Lees KR, Lyden P, Grotta J, Davalos A, Davis SM, Shuaib A, Ashwood T, Wasiewski W, Alderfer V, Hardemark HG, Rodichok L (2008) NXY-059 for the treatment of acute stroke: pooled analysis of the SAINT I and II trials. *Stroke* 39:1751–8

Dijkhuizen RM, Ren J, Mandeville JB, Wu O, Ozdag FM, Moskowitz MA, Rosen BR, Finklestein SP (2001) Functional magnetic resonance imaging of reorganization in rat brain after stroke. *Proc Natl Acad Sci USA* 98:12766–71

Dirnagl U (2006) Bench to bedside: the quest for quality in experimental stroke research. *J Cereb Blood Flow Metab* 26:1465–78

Dittmar MS, Fehm NP, Vatankhah B, Bogdahn U, Schlachetzki F (2005) Adverse effects of the intraluminal filament model of middle cerebral artery occlusion. *Stroke* 36:530–2; author reply 532

Donnan GA, Baron JC, Ma H, Davis SM (2009) Penumbral selection of patients for trials of acute stroke therapy. *Lancet Neurol* 8:261–9

Farr TD, Carswell HV, Gsell W, Macrae IM (2007) Estrogen receptor beta agonist diarylpropiolnitrile (DPN) does not mediate neuroprotection in a rat model of permanent focal ischemia. *Brain Res* 1185:275–82

Felberg RA, Okon NJ, El-Mitwalli A, Burgin WS, Grotta JC, Alexandrov AV (2002) Early dramatic recovery during intravenous tissue plasminogen activator infusion: clinical pattern and outcome in acute middle cerebral artery stroke. *Stroke* 33:1301–7

Fiebach JB, Schellinger PD (2009) MR mismatch is useful for patient selection for thrombolysis: yes. *Stroke* 40:2906–7

Fiehler J, Albers GW, Boulanger JM, Derex L, Gass A, Hjort N, Kim JS, Liebeskind DS, Neumann-Haefelin T, Pedraza S, Rother J, Rothwell P, Rovira A, Schellinger PD, Trenkler J (2007) Bleeding Risk Analysis in Stroke Imaging before thromboLysis (BRASIL): pooled analysis of T2*-weighted magnetic resonance imaging data from 570 patients. *Stroke* 38:2738–44

Garcia JH, Wagner S, Liu KF, Hu XJ (1995) Neurological deficit and extent of neuronal necrosis attributable to middle cerebral artery occlusion in rats. Statistical validation. *Stroke* 26:627–34; discussion 35

Gerriets T, Stolz E, Walberer M, Muller C, Rottger C, Kluge A, Kaps M, Fisher M, Bachmann G (2004) Complications and pitfalls in rat stroke models for middle cerebral artery occlusion: a comparison between the suture and the macrosphere model using magnetic resonance angiography. *Stroke* 35:2372–7

Goldberg M. Stroke Trials Registry. Internet Stroke Center. www.strokecenter.org

Granziera C, D'Arceuil H, Zai L, Magistretti PJ, Sorensen AG, de Crespigny AJ (2007) Long-term monitoring of post-stroke plasticity after transient cerebral ischemia in mice using *in vivo* and *ex vivo* diffusion tensor MRI. *Open Neuroimag J* 1:10–7

Grefkes C, Fink GR (2009) Functional reorganization and neuromodulation. In: *Sensorimotor Control of Grasping: Physiology and Pathophysiology* (Nowak DA, Hermsdörfer J, eds), Cambridge University Press: UK, 425–437

Guadagno JV, Warburton EA, Aigbirhio FI, Smielewski P, Fryer TD, Harding S, Price CJ, Gillard JH, Carpenter TA, Baron JC (2004) Does the acute diffusion-weighted imaging lesion represent penumbra as well as core? A

combined quantitative PET/MRI voxel-based study. *J Cereb Blood Flow Metab* 24:1249–54

Guadagno JV, Jones PS, Fryer TD, Barret O, Aigbirhio FI, Carpenter TA, Price CJ, Gillard JH, Warburton EA, Baron JC (2006) Local relationships between restricted water diffusion and oxygen consumption in the ischemic human brain. *Stroke* 37:1741–8

Hacke W, Kaste M, Bluhmki E, Brozman M, Davalos A, Guidetti D, Larrue V, Lees KR, Medeghri Z, Machnig T, Schneider D, von Kummer R, Wahlgren N, Toni D (2008) Thrombolysis with alteplase 3 to 4.5 h after acute ischemic stroke. *N Engl J Med* 359:1317–29

Hacke W, Furlan AJ, Al-Rawi Y, Davalos A, Fiebach JB, Gruber F, Kaste M, Lipka LJ, Pedraza S, Ringleb PA, Rowley HA, Schneider D, Schwamm LH, Leal JS, Sohngen M, Teal PA, Wilhelm-Ogunbiyi K, Wintermark M, Warach S (2009) Intravenous desmoteplase in patients with acute ischaemic stroke selected by MRI perfusion–diffusion weighted imaging or perfusion CT (DIAS-2): a prospective, randomised, double-blind, placebo-controlled study. *Lancet Neurol* 8:141–50

Hand PJ, Wardlaw JM, Rivers CS, Armitage PA, Bastin ME, Lindley RI, Dennis MS (2006) MR diffusion-weighted imaging and outcome prediction after ischemic stroke. *Neurology* 66:1159–63

Heiss WD, Sobesky J, Smekal U, Kracht LW, Lehnhardt FG, Thiel A, Jacobs AH, Lackner K (2004) Probability of cortical infarction predicted by flumazenil binding and diffusion-weighted imaging signal intensity: a comparative positron emission tomography/magnetic resonance imaging study in early ischemic stroke. *Stroke* 35:1892–8

Hendrikse J, Petersen ET, Cheze A, Chng SM, Venketasubramanian N, Golay X (2009) Relation between cerebral perfusion territories and location of cerebral infarcts. *Stroke* 40:1617–22

Henning EC, Ruetzler CA, Gaudinski MR, Hu TC, Latour LL, Hallenbeck JM, Warach S (2009) Feridex preloading permits tracking of CNS-resident macrophages after transient middle cerebral artery occlusion. *J Cereb Blood Flow Metab* 29:1229–39

Henninger N, Sicard KM, Schmidt KF, Bardutzky J, Fisher M (2006) Comparison of ischemic lesion evolution in embolic versus mechanical middle cerebral artery occlusion in Sprague Dawley rats using diffusion and perfusion imaging. *Stroke* 37:1283–7

Hilger T, Niessen F, Diedenhofen M, Hossmann KA, Hoehn M (2002) Magnetic resonance angiography of thromboembolic stroke in rats: indicator of recanalization probability and tissue survival after recombinant tissue plasminogen activator treatment. *J Cereb Blood Flow Metab* 22:652–62

Hsia AW, Sachdev HS, Tomlinson J, Hamilton SA, Tong DC (2003) Efficacy of IV tissue plasminogen activator in acute stroke: does stroke subtype really matter? *Neurology* 61:71–5

Hwang YH, Seo JG, Lee HW, Park SP, Suh CK (2008) Early neurological deterioration following intravenous recombinant tissue plasminogen activator therapy in patients with acute lacunar stroke. *Cerebrovasc Dis* 26:355–9

Jacobs MA, Knight RA, Soltanian-Zadeh H, Zheng ZG, Goussev AV, Peck DJ, Windham JP, Chopp M (2000) Unsupervised segmentation of multiparameter MRI in experimental cerebral ischemia with comparison to T2, diffusion, and ADC MRI parameters and histopathological validation. *J Magn Reson Imaging* 11:425–37

Jiang Q, Zhang ZG, Ding GL, Silver B, Zhang L, Meng H, Lu M, Pourabdillah-Nejed DS, Wang L, Savant-Bhonsale S, Li L, Bagher-Ebadian H, Hu J, Arbab AS, Vanguri P, Ewing JR, Ledbetter KA, Chopp M (2006) MRI detects white matter reorganization after neural progenitor cell treatment of stroke. *Neuroimage* 32:1080–9

Johnston KC, Barrett KM, Ding YH, Wagner DP (2009) Clinical and imaging data at 5 days as a surrogate for 90-day outcome in ischemic stroke. *Stroke* 40:1332–3

Jorgensen HS, Sperling B, Nakayama H, Raaschou HO, Olsen TS (1994) Spontaneous reperfusion of cerebral infarcts in patients with acute stroke. Incidence, time course, and clinical outcome in the Copenhagen Stroke Study. *Arch Neurol* 51:865–73

Judenhofer MS, Wehrl HF, Newport DF, Catana C, Siegel SB, Becker M, Thielscher A, Kneilling M, Lichy MP, Eichner M, Klingel K, Reischl G, Widmaier S, Rocken M, Nutt RE, Machulla HJ, Uludag K, Cherry SR, Claussen CD, Pichler BJ (2008) Simultaneous PET-MRI: a new approach for functional and morphological imaging. *Nat Med* 14:459–65

Kane I, Sandercock P, Wardlaw J (2007) Magnetic resonance perfusion diffusion mismatch and thrombolysis in acute ischaemic stroke: a systematic review of the evidence to date. *J Neurol Neurosurg Psychiatry* 78:485–91

Kasner SE (2006) Clinical interpretation and use of stroke scales. *Lancet Neurol* 5:603–12

Kazemi M, Silva MD, Li F, Fisher M, Sotak CH (2004) Investigation of techniques to quantify *in vivo* lesion volume based on comparison of water apparent diffusion coefficient (ADC) maps with histology in focal cerebral ischemia of rats. *Magn Reson Imaging* 22:653–9

Kidwell CS, Chalela JA, Saver JL, Starkman S, Hill MD, Demchuk AM, Butman JA, Patronas N, Alger JR, Latour LL, Luby ML, Baird AE, Leary MC, Tremwel M, Ovbiagele B, Fredieu A, Suzuki S, Villablanca JP, Davis S, Dunn B, Todd JW, Ezzeddine MA, Haymore J, Lynch JK, Davis L, Warach S (2004) Comparison of MRI and CT for detection of acute intracerebral hemorrhage. *JAMA* 292:1823–30

Kimura K, Iguchi Y, Shibazaki K, Aoki J, Uemura J (2009) Early recanalization rate of major occluded brain arteries after intravenous tissue plasminogen activator therapy using serial magnetic resonance angiography studies. *Eur Neurol* 62:287–92

Kleindorfer D, Kissela B, Schneider A, Woo D, Khoury J, Miller R, Alwell K, Gebel J, Szaflarski J, Pancioli A, Jauch E, Moomaw C, Shukla R, Broderick JP (2004) Eligibility for recombinant tissue plasminogen activator in acute ischemic stroke: a population-based study. *Stroke* 35:e27–9

Kooi ME, Cappendijk VC, Cleutjens KB, Kessels AG, Kitslaar PJ, Borgers M, Frederik PM, Daemen MJ, van Engelshoven JM (2003) Accumulation of ultrasmall superparamagnetic particles of iron oxide in human atherosclerotic plaques can be detected by *in vivo* magnetic resonance imaging. *Circulation* 107:2453–8

Kraemer N, Thomalla G, Soennichsen J, Fiehler J, Knab R, Kucinski T, Zeumer H, Rother J (2005) Magnetic resonance imaging and clinical patterns of patients with 'spectacular shrinking deficit' after acute middle cerebral artery stroke. *Cerebrovasc Dis* 20:285–90

Kuker W, Gaertner S, Nagele T, Dopfer C, Schoning M, Fiehler J, Rothwell PM, Herrlinger U (2008) Vessel wall contrast enhancement: a diagnostic sign of cerebral vasculitis. *Cerebrovasc Dis* 26:23–9

Latchaw RE, Alberts MJ, Lev MH, Connors JJ, Harbaugh RE, Higashida RT, Hobson R, Kidwell CS, Koroshetz WJ, Mathews V, Villablanca P, Warach S, Walters B (2009) Recommendations for imaging of acute ischemic stroke. A scientific statement from the American Heart Association. *Stroke* 40:3646–78

Lefkowitz D, LaBenz M, Nudo SR, Steg RE, Bertoni JM (1999) Hyperacute ischemic stroke missed by diffusion-weighted imaging. *AJNR Am J Neuroradiol* 20:1871–5

Leithner C, Gertz K, Schrock H, Priller J, Prass K, Steinbrink J, Villringer A, Endres M, Lindauer U, Dirnagl U, Royl G (2008) A flow sensitive alternating inversion recovery (FAIR)-MRI protocol to measure hemispheric cerebral blood flow in a mouse stroke model. *Exp Neurol* 210:118–27

Li F, Silva MD, Liu KF, Helmer KG, Omae T, Fenstermacher JD, Sotak CH, Fisher M (2000) Secondary decline in apparent diffusion coefficient and neurological outcomes after a short period of focal brain ischemia in rats. *Ann Neurol* 48:236–44

Liu KF, Li F, Tatlisumak T, Garcia JH, Sotak CH, Fisher M, Fenstermacher JD (2001) Regional variations in the apparent diffusion coefficient and the intracellular distribution of water in rat brain during acute focal ischemia. *Stroke* 32:1897–905

Lorenz C, Benner T, Lopez CJ, Ay H, Zhu MW, Aronen H, Karonen J, Liu Y, Nuutinen J, Sorensen AG (2006) Effect of using local arterial input functions on cerebral blood flow estimation. *J Magn Reson Imaging* 24:57–65

Mandeville JB, Marota JJ, Kosofsky BE, Keltner JR, Weissleder R, Rosen BR, Weisskoff RM (1998) Dynamic functional imaging of relative cerebral blood volume during rat forepaw stimulation. *Magn Reson Med* 39:615–24

Masdeu JC, Irimia P, Asenbaum S, Bogousslavsky J, Brainin M, Chabriat H, Herholz K, Markus HS, Martinez-Vila E, Niederkorn K, Schellinger PD, Seitz RJ (2006) EFNS guideline on neuroimaging in acute stroke. Report of an EFNS task force. *Eur J Neurol* 13:1271–83

Meng X, Fisher M, Shen Q, Sotak CH, Duong TQ (2004) Characterizing the diffusion/perfusion mismatch in experimental focal cerebral ischemia. *Ann Neurol* 55:207–12

Mitsumori LM, Hatsukami TS, Ferguson MS, Kerwin WS, Cai J, Yuan C (2003) *In vivo* accuracy of multisequence MR imaging for identifying unstable fibrous caps in advanced human carotid plaques. *J Magn Reson Imaging* 17:410–20

Moller M, Frandsen J, Andersen G, Gjedde A, Vestergaard-Poulsen P, Ostergaard L (2007) Dynamic changes in corticospinal tracts after stroke detected by fibretracking. *J Neurol Neurosurg Psychiatry* 78:587–92

Montoya CP, Campbell-Hope LJ, Pemberton KD, Dunnett SB (1991) The 'staircase test': a measure of independent forelimb reaching and grasping abilities in rats. *J Neurosci Methods* 36:219–28

Morita N, Harada M, Uno M, Furutani K, Nishitani H (2006) Change of diffusion anisotropy in patients with acute cerebral infarction using statistical parametric analysis. *Radiat Med* 24:253–9

Na DG, Thijs VN, Albers GW, Moseley ME, Marks MP (2004) Diffusion-weighted MR imaging in acute ischemia: value of apparent diffusion coefficient and signal intensity thresholds in predicting tissue at risk and final infarct size. *AJNR Am J Neuroradiol* 25:1331–6

National Institute of Neurological Disorders Stroke rt-PA Stroke Study Group (2005) Recombinant tissue plasminogen activator for minor strokes: the National Institute of Neurological Disorders and Stroke rt-PA Stroke Study experience. *Ann Emerg Med* 46:243–52

Nederkoorn PJ, Elgersma OE, van der Graaf Y, Eikelboom BC, Kappelle LJ, Mali WP (2003) Carotid artery stenosis: accuracy of contrast-enhanced MR angiography for diagnosis. *Radiology* 228:677–82

Neumann-Haefelin T, Wittsack HJ, Wenserski F, Siebler M, Seitz RJ, Modder U, Freund HJ (1999) Diffusion- and perfusion-weighted MRI. The DWI/PWI mismatch region in acute stroke. *Stroke* 30:1591–7

Neumann-Haefelin T, Kastrup A, de Crespigny A, Yenari MA, Ringer T, Sun GH, Moseley ME (2000) Serial MRI after transient focal cerebral ischemia in rats: dynamics of tissue injury, blood–brain barrier damage, and edema formation. *Stroke* 31:1965–72; discussion 72–3

Neumann-Haefelin T, Kastrup A, de Crespigny A, Ringer TM, Sun GH, Yenari MA, Moseley ME (2001) MRI of subacute hemorrhagic transformation in the rat suture occlusion model. *Neuroreport* 12:309–11

Neumann-Haefelin T, du Mesnil de Rochemont R, Fiebach JB, Gass A, Nolte C, Kucinski T, Rother J, Siebler M, Singer OC, Szabo K, Villringer A, Schellinger PD (2004) Effect of incomplete (spontaneous and post-thrombolytic) recanalization after middle cerebral artery occlusion: a magnetic resonance imaging study. *Stroke* 35:109–14

Neumann AB, Jonsdottir KY, Mouridsen K, Hjort N, Gyldensted C, Bizzi A, Fiehler J, Gasparotti R, Gillard JH, Hermier M, Kucinski T, Larsson EM, Sorensen L, Ostergaard L (2009) Interrater agreement for final infarct MRI lesion delineation. *Stroke* 40:3768–71

Nighoghossian N, Hermier M, Adeleine P, Blanc-Lasserre K, Derex L, Honnorat J, Philippeau F, Dugor JF, Froment JC, Trouillas P (2002) Old microbleeds are a potential risk factor for cerebral bleeding after ischemic stroke: a gradient-echo T2*-weighted brain MRI study. *Stroke* 33:735–42

Nighoghossian N, Wiart M, Cakmak S, Berthezene Y, Derex L, Cho TH, Nemoz C, Chapuis F, Tisserand GL, Pialat JB, Trouillas P, Froment JC, Hermier M (2007) Inflammatory response after ischemic stroke: a USPIO-enhanced MRI study in patients. *Stroke* 38:303–7

Nonent M, Serfaty JM, Nighoghossian N, Rouhart F, Derex L, Rotaru C, Chirossel P, Guias B, Heautot JF, Gouny P, Langella B, Buthion V, Jars I, Pachai C, Veyret C, Gauvrit JY, Lamure M, Douek PC (2004) Concordance rate differences of 3 noninvasive imaging techniques to measure carotid stenosis in clinical routine practice: results of the CARMEDAS multicenter study. *Stroke* 35:682–6

Olah L, Wecker S, Hoehn M (2001) Relation of apparent diffusion coefficient changes and metabolic disturbances after 1 h of focal cerebral ischemia and at different reperfusion phases in rats. *J Cereb Blood Flow Metab* 21:430–9

Olivot JM, Mlynash M, Thijs VN, Kemp S, Lansberg MG, Wechsler L, Bammer R, Marks MP, Albers GW (2009) Optimal Tmax threshold for predicting penumbral tissue in acute stroke. *Stroke* 40:469–75

Ostergaard L (2005) Principles of cerebral perfusion imaging by bolus tracking. *J Magn Reson Imaging* 22:710–7

Ozsunar Y, Koseoglu K, Huisman TA, Koroshetz W, Sorensen AG (2004) MRI measurements of water diffusion: impact of region of interest selection on ischemic quantification. *Eur J Radiol* 51:195–201

Paciaroni M, Caso V, Agnelli G (2009) The concept of ischemic penumbra in acute stroke and therapeutic opportunities. *Eur Neurol* 61:321–30

Palmer GC, Peeling J, Corbett D, Del Bigio MR, Hudzik TJ (2001) T2-weighted MRI correlates with long-term histopathology, neurology scores, and skilled motor behavior in a rat stroke model. *Ann NY Acad Sci* 939:283–96

Pannek K, Chalk JB, Finnigan S, Rose SE (2009) Dynamic corticospinal white matter connectivity changes during stroke recovery: a diffusion tensor probabilistic tractography study. *J Magn Reson Imaging* 29:529–36

Rausch M, Baumann D, Neubacher U, Rudin M (2002) *In-vivo* visualization of phagocytotic cells in rat brains after transient ischemia by USPIO. *NMR Biomed* 15:278–83

Ren H, Shen Q, Bardutzky J, Fisher M, Duong TQ (2004) Partial-volume effect on ischemic tissue-fate delineation using quantitative perfusion and diffusion imaging on a rat stroke model. *Magn Reson Med* 52:1328–35

Ricci PE, Burdette JH, Elster AD, Reboussin DM (1999) A comparison of fast spin-echo, fluid-attenuated inversion-recovery, and diffusion-weighted MR imaging in the first 10 days after cerebral infarction. *AJNR Am J Neuroradiol* 20:1535–42

Ringer TM, Neumann-Haefelin T, Sobel RA, Moseley ME, Yenari MA (2001) Reversal of early diffusion-weighted magnetic resonance imaging abnormalities does not necessarily reflect tissue salvage in experimental cerebral ischemia. *Stroke* 32:2362–9

Rivers CS, Wardlaw JM (2005) What has diffusion imaging in animals told us about diffusion imaging in patients with ischaemic stroke? *Cerebrovasc Dis* 19:328–36

Roberts HC, Dillon WP, Furlan AJ, Wechsler LR, Rowley HA, Fischbein NJ, Higashida RT, Kase C, Schulz GA, Lu Y, Firszt CM (2002) Computed tomographic findings in patients undergoing intra-arterial thrombolysis for acute ischemic stroke due to middle cerebral artery occlusion: results from the PROACT II trial. *Stroke* 33:1557–65

Rosso C, Hevia-Montiel N, Deltour S, Bardinet E, Dormont D, Crozier S, Baillet S, Samson Y (2009) Prediction of infarct growth based on apparent diffusion coefficients: penumbral assessment without intravenous contrast material. *Radiology* 250:184–92

Rother J, Schellinger PD, Gass A, Siebler M, Villringer A, Fiebach JB, Fiehler J, Jansen O, Kucinski T, Schoder V, Szabo K, Junge-Hulsing GJ, Hennerici M, Zeumer H, Sartor K, Weiller C, Hacke W (2002) Effect of intravenous thrombolysis on MRI parameters and functional outcome in acute stroke <6 h. *Stroke* 33:2438–45

Saam T, Hatsukami TS, Takaya N, Chu B, Underhill H, Kerwin WS, Cai J, Ferguson MS, Yuan C (2007) The vulnerable, or high-risk, atherosclerotic plaque: noninvasive MR imaging for characterization and assessment. *Radiology* 244:64–77

Saleh A, Schroeter M, Ringelstein A, Hartung HP, Siebler M, Modder U, Jander S (2007) Iron oxide particle-enhanced MRI suggests variability of brain inflammation at early stages after ischemic stroke. *Stroke* 38:2733–7

Schabitz WR (2009) MR mismatch is useful for patient selection for thrombolysis: no. *Stroke* 40:2908–9

Schallert T, Fleming SM, Leasure JL, Tillerson JL, Bland ST (2000) CNS plasticity and assessment of forelimb sensorimotor outcome in unilateral rat models of stroke, cortical ablation, parkinsonism and spinal cord injury. *Neuropharmacology* 39:777–87

Schiemanck SK, Kwakkel G, Post MW, Prevo AJ (2006) Predictive value of ischemic lesion volume assessed with magnetic resonance imaging for neurological deficits and functional outcome poststroke: a critical review of the literature. *Neurorehabil Neural Repair* 20:492–502

Sharp FR, Lu A, Tang Y, Millhorn DE (2000) Multiple molecular penumbras after focal cerebral ischemia. *J Cereb Blood Flow Metab* 20:1011–32

Shen Q, Meng X, Fisher M, Sotak CH, Duong TQ (2003) Pixel-by-pixel spatiotemporal progression of focal ischemia derived using quantitative perfusion and diffusion imaging. *J Cereb Blood Flow Metab* 23:1479–88

Shen Q, Fisher M, Sotak CH, Duong TQ (2004) Effects of reperfusion on ADC and CBF pixel-by-pixel dynamics in stroke: characterizing tissue fates using quantitative diffusion and perfusion imaging. *J Cereb Blood Flow Metab* 24:280–90

Silva AC, Lee SP, Yang G, Iadecola C, Kim SG (1999) Simultaneous blood oxygenation level-dependent and cerebral blood flow functional magnetic resonance imaging during forepaw stimulation in the rat. *J Cereb Blood Flow Metab* 19:871–9

Sims JR, Gharai LR, Schaefer PW, Vangel M, Rosenthal ES, Lev MH, Schwamm LH (2009) ABC/2 for rapid clinical estimate of infarct, perfusion, and mismatch volumes. *Neurology* 72:2104–10

Sobesky J, Zaro Weber O, Lehnhardt FG, Hesselmann V, Thiel A, Dohmen C, Jacobs A, Neveling M, Heiss WD (2004) Which time-to-peak threshold best identifies penumbral flow? A comparison of perfusion-weighted magnetic resonance imaging and positron emission tomography in acute ischemic stroke. *Stroke* 35:2843–7

Sobesky J, Zaro Weber O, Lehnhardt FG, Hesselmann V, Neveling M, Jacobs A, Heiss WD (2005) Does the mismatch match the penumbra? Magnetic resonance imaging and positron emission tomography in early ischemic stroke. *Stroke* 36:980–5

Stinear CM, Barber PA, Smale PR, Coxon JP, Fleming MK, Byblow WD (2007) Functional potential in chronic stroke patients depends on corticospinal tract integrity. *Brain* 130:170–80

Sulter G, Steen C, De Keyser J (1999) Use of the Barthel index and modified Rankin scale in acute stroke trials. *Stroke* 30:1538–41

Sun PZ, Zhou J, Sun W, Huang J, van Zijl PC (2007) Detection of the ischemic penumbra using pH-weighted MRI. *J Cereb Blood Flow Metab* 27:1129–36

Takasawa M, Jones PS, Guadagno JV, Christensen S, Fryer TD, Harding S, Gillard JH, Williams GB, Aigbirhio FI, Warburton EA, Ostergaard L, Baron JC (2008) How reliable is perfusion MR in acute stroke? Validation and determination of the penumbra threshold against quantitative PET. *Stroke* 39:870–7

Thomalla GJ, Kucinski T, Schoder V, Fiehler J, Knab R, Zeumer H, Weiller C, Rother J (2003) Prediction of malignant middle cerebral artery infarction by early perfusion- and diffusion-weighted magnetic resonance imaging. *Stroke* 34:1892–9

Uchino K, Alexandrov AV, Garami Z, El-Mitwalli A, Morgenstern LB, Grotta JC (2005) Safety and feasibility of a lower dose intravenous TPA therapy for ischemic stroke beyond the first three hours. *Cerebrovasc Dis* 19:260–6

van der Zijden JP, van der Toorn A, van der Marel K, Dijkhuizen RM (2008) Longitudinal *in vivo* MRI of

alterations in perilesional tissue after transient ischemic stroke in rats. *Exp Neurol* 212:207–12
van Laar PJ, van der Grond J, Hendrikse J (2008) Brain perfusion territory imaging: methods and clinical applications of selective arterial spin-labeling MR imaging. *Radiology* 246:354–64
Villringer A, Rosen BR, Belliveau JW, Ackerman JL, Lauffer RB, Buxton RB, Chao YS, Wedeen VJ, Brady TJ (1988) Dynamic imaging with lanthanide chelates in normal brain: contrast due to magnetic susceptibility effects. *Magn Reson Med* 6:164–74
von Kummer R (2002) Brain hemorrhage after thrombolysis: good or bad? *Stroke* 33:1446–7
Wang PY, Barker PB, Wityk RJ, Ulug AM, van Zijl PC, Beauchamp Jr NJ (1999) Diffusion-negative stroke: a report of two cases. *AJNR Am J Neuroradiol* 20:1876–80
Warach S, Pettigrew LC, Dashe JF, Pullicino P, Lefkowitz DM, Sabounjian L, Harnett K, Schwiderski U, Gammans R (2000) Effect of citicoline on ischemic lesions as measured by diffusion-weighted magnetic resonance imaging. Citicoline 010 Investigators. *Ann Neurol* 48:713–22
Wardlaw JM, Keir SL, Bastin ME, Armitage PA, Rana AK (2002) Is diffusion imaging appearance an independent predictor of outcome after ischemic stroke? *Neurology* 59:1381–7
Warlow C, Sudlow C, Dennis M, Wardlaw J, Sandercock P (2003) Stroke. *Lancet* 362:1211–24
Weber R, Ramos-Cabrer P, Justicia C, Wiedermann D, Strecker C, Sprenger C, Hoehn M (2008) Early prediction of functional recovery after experimental stroke: functional magnetic resonance imaging, electrophysiology, and behavioral testing in rats. *J Neurosci* 28:1022–9
Wegener S, Wu WC, Perthen JE, Wong EC (2007) Quantification of rodent cerebral blood flow (CBF) in normal and high flow states using pulsed arterial spin labeling magnetic resonance imaging. *J Magn Reson Imaging* 26:855–62
Whishaw IQ, Pellis SM, Gorny BP (1992) Skilled reaching in rats and humans: evidence for parallel development or homology. *Behav Brain Res* 47:59–70
Wiart M, Davoust N, Pialat JB, Desestret V, Moucharaffie S, Cho TH, Mutin M, Langlois JB, Beuf O, Honnorat J, Md NN, Berthezene Y (2007) MRI monitoring of neuroinflammation in mouse focal ischemia. *Stroke* 38:131–7
Williams DS, Detre JA, Leigh JS, Koretsky AP (1992) Magnetic resonance imaging of perfusion using spin inversion of arterial water. *Proc Natl Acad Sci USA* 89:212–6
Wong EC (2007) Vessel-encoded arterial spin-labeling using pseudocontinuous tagging. *Magn Reson Med* 58:1086–91
Xu F, Ge Y, Lu H (2009) Noninvasive quantification of whole-brain cerebral metabolic rate of oxygen ($CMRO_2$) by MRI. *Magn Reson Med* 62:141–8
Yim YJ, Choe YH, Ko Y, Kim ST, Kim KH, Jeon P, Byun HS, Kim DI (2008) High signal intensity halo around the carotid artery on maximum intensity projection images of time-of-flight MR angiography: a new sign for intraplaque hemorrhage. *J Magn Reson Imaging* 27:1341–6
Yu D, Schaefer PW, Rordorf G, Gonzalez RG (2002) Magnetic resonance angiography in acute stroke. *Semin Roentgenol* 37:212–8
Zaro-Weber O, Moeller-Hartmann W, Heiss WD, Sobesky J (2009) The performance of MRI-based cerebral blood flow measurements in acute and subacute stroke compared with 15O-water positron emission tomography. Identification of penumbral flow. *Stroke* 40:2413–21
Zelaya F, Flood N, Chalk JB, Wang D, Doddrell DM, Strugnell W, Benson M, Ostergaard L, Semple J, Eagle S (1999) An evaluation of the time dependence of the anisotropy of the water diffusion tensor in acute human ischemia. *Magn Reson Imaging* 17:331–48